



Measurement of direct CP violation in $B^+ \rightarrow J/\psi K^+$ decay

The DØ Collaboration
URL: <http://www-d0.fnal.gov>
(Dated: July 17, 2007)

We have performed a measurement of direct CP violation in the $b \rightarrow c\bar{c}s$ transitions by searching for a charge asymmetry in the decay $B^\pm \rightarrow J/\psi K^\pm$. The event sample was selected from 1.6 fb^{-1} of data collected by the DØ experiment in Run II of the Tevatron collider at Fermilab. We obtain $A_{CP}(B^+ \rightarrow J/\psi K^+) = +0.0067 \pm 0.0074(\text{stat}) \pm 0.0026(\text{syst})$, which is consistent with the Standard Model expectation.

I. MOTIVATION

The $B^\pm \rightarrow J/\psi K^\pm$ decay proceeds through the quark decay $b \rightarrow c\bar{c}s$ and its conjugate process. The Standard Model predicts a small direct CP violation in this decay channel mainly due to the interference between direct (Fig. 1, a) and annihilation (Fig. 1, b) amplitudes.

CP violation manifests itself as a decay rate asymmetry between the $b \rightarrow c\bar{c}s$ decay and its conjugate:

$$A_{CP}(B^+ \rightarrow J/\psi(1S)K^+) = \frac{\Gamma(B^- \rightarrow J/\psi K^-) - \Gamma(B^+ \rightarrow J/\psi K^+)}{\Gamma(B^- \rightarrow J/\psi K^-) + \Gamma(B^+ \rightarrow J/\psi K^+)}. \quad (1)$$

In the Standard Model, $A_{CP}(B^+ \rightarrow J/\psi(1S)K^+)$ is predicted to be at the level of 1% [1]. However, there are theoretical models which predict an enhanced asymmetry in this channel because of the additional phases arising due to the new physics couplings at tree level. Most cited are the model with an extra $U(1)'$ gauge boson responsible for the flavor-changing coupling between b and s quarks [2] and the Two-Higgs Doublet Model (THDM) which introduces an extra coupling to the charged Higgs [3].

To measure the $A_{CP}(B^+ \rightarrow J/\psi K^+)$, neither tagging nor time-dependence measurements are required, it is enough to measure the charge asymmetry between $B^- \rightarrow J/\psi K^-$ and $B^+ \rightarrow J/\psi K^+$ using the kaon charge as a tag. Also, the clean experimental signature of the final state due to the charmonium decay and the large branching ratio of $\sim 10^{-3}$ make the selection of the event sample fairly straightforward.

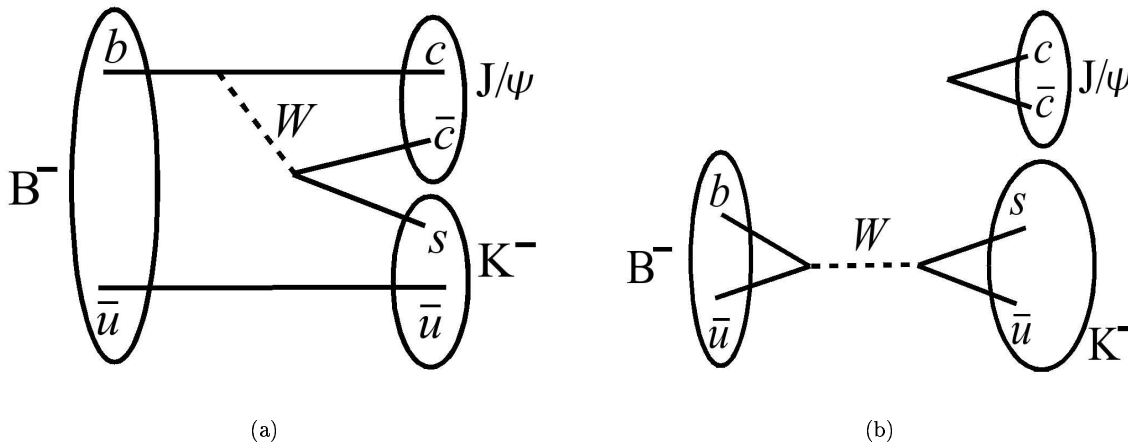


FIG. 1: Leading amplitudes for the $B^\pm \rightarrow J/\psi K^\pm$ decay: direct (a) and annihilation (b). For the annihilation amplitude gluons are not shown (there should be at least three for J/ψ).

II. DETECTOR DESCRIPTION

This measurement was performed using a large sample of B^\pm decays collected by the $D\mathcal{O}$ experiment at the Fermilab Tevatron collider in $p\bar{p}$ collisions at center-of-mass energy $\sqrt{s} = 1.96$ TeV. The $D\mathcal{O}$ detector is described in detail elsewhere [4]. The detector components most important to this analysis are the central tracking and muon systems. The central tracking system consists of a silicon microstrip tracker (SMT) and a central fiber tracker (CFT), both located within a 2 T superconducting solenoidal magnet, with designs optimized for tracking and vertexing for pseudorapidities of $|\eta| < 3$ and $|\eta| < 2.5$, respectively. An outer muon system, with coverage for $|\eta| < 2$, consists of a layer of tracking detectors and scintillation trigger counters in front of 1.8 T toroids, followed by two similar layers after the toroids [5]. The polarities of the solenoid and toroids are regularly reversed during data taking, so that the four solenoid-toroid polarity combinations are exposed to approximately the same integrated luminosity. The forward and reverse polarity magnetic fields in the magnets were measured to be equal to within 0.1%. The reversal of magnet polarities is essential to reduce the detector-related systematics in charge asymmetry measurements to the necessary level, and is fully exploited in this analysis.

III. $B \rightarrow J/\psi K$ SAMPLE SELECTION

The event sample was collected using di-muon triggers. The B^+ meson was reconstructed in the exclusive decay $B^+ \rightarrow J/\psi K^+$ with J/ψ decaying to $\mu^+\mu^-$. Each muon was required to be identified by the muon system, to have an associated track in the central tracking system with at least two measurements in the SMT, and a transverse momentum $p_T^\mu > 1.5$ GeV/ c . At least one of the two muons was required to have matching track segments both inside and outside the toroidal magnet. The two muons must form a common vertex and have an invariant mass between 2.8 and 3.35 GeV/ c^2 , to form a J/ψ candidate. An additional charged track with $p_T > 0.5$ GeV/ c , with total momentum above 0.7 GeV/ c and with at least two measurements in the SMT, was selected. This particle was assigned the mass of the kaon mass and was required to have a common vertex, with $\chi^2 < 16$ for 3 degrees of freedom, with the two muons. The displacement of this vertex from the primary interaction point was required to exceed three standard deviations in the plane perpendicular to the beam direction. The primary vertex of the $p\bar{p}$ interaction was determined for each event using the method described in Ref. [6]. The average position of the beam-collision point was included as a constraint.

From each set of three particles fulfilling these requirements, a B^+ candidate was constructed. The momenta of the muons were corrected using the J/ψ mass constraint. To further improve the B^+ selection, a likelihood ratio method [7] was utilized. This method provides a simple way of combining several discriminating variables into a single variable with increased power to separate signal and background. The variables chosen for this analysis include the lower transverse momentum of the two muons, the χ^2 of the B^+ decay vertex, the B^+ decay length divided by its error, the significance (defined below) S_B of the B^+ track impact parameter (IP), the transverse momentum of the kaon, and the significance S_K of the kaon track impact parameter.

For any track i , the IP significance was defined as $S_i = \sqrt{[\epsilon_T/\sigma(\epsilon_T)]^2 + [\epsilon_L/\sigma(\epsilon_L)]^2}$, where ϵ_T (ϵ_L) is the projection of the track impact parameter on the plane perpendicular to the beam direction (along the beam direction), and $\sigma(\epsilon_T)$ [$\sigma(\epsilon_L)$] is its uncertainty. The track of each B^+ was formed assuming that it passes through the reconstructed vertex and is directed along the reconstructed B^+ momentum.

Finally the mass of the reconstructed B^+ candidate was constrained to the window $4.98 < M(\mu\mu K) < 5.76$ GeV/ c^2 . The mass range was chosen wide enough to include the sidebands to ensure a stable description of the background under the peak during the mass modeling.

IV. MASS MODELING

The resulting invariant mass distribution of the $J/\psi K$ system is shown in Fig. 2. The curve represents the result of an unbinned likelihood fit to the sum of contributions from $B \rightarrow J/\psi K$, $B \rightarrow J/\psi\pi$, and $B \rightarrow J/\psi K^*$ decays, as well as combinatorial background. The mass distribution of the $J/\psi K$ system from the $B \rightarrow J/\psi K$ hypothesis was parameterized by a Gaussian with the width depending on the momentum of the K^+ . The mass distribution of the $J/\psi\pi$ system from the $B \rightarrow J/\psi\pi$ hypothesis was parameterized by a Gaussian with the same width. It is then transformed into the distribution of the $J/\psi K$ system by assigning the kaon mass to the pion. The decay $B \rightarrow J/\psi K^*$ with $K^* \rightarrow K\pi$, where pion is not reconstructed, produces a broad $J/\psi K^+$ mass distribution with the threshold near $M(B) - M(\pi)$. It was parameterized using the Monte Carlo simulation. The combinatorial background (BKG) was described by an exponential function. The dependence of the fractions of $J/\psi K$, $J/\psi\pi$, and $J/\psi K^*$ events on the kaon momentum was verified to be the same in the simulation. It was parameterised by a polynomial with coefficients determined from the fit.

The number of events in each channel is summarized in Table I. Note, that as both $J/\psi K$ and $J/\psi\pi$ signals fall into the mass fit window, we should expect the ratio of the numbers of events in the $J/\psi\pi$ and $J/\psi K$ channels to correspond to the ratio of the $J/\psi\pi$ and $J/\psi K$ branching fractions [8]. Indeed, from Table I we obtain $N(J/\psi\pi)/N(J/\psi K) = [4.06 \pm 0.35(stat)] \times 10^{-2}$, which is confirmed by the PDG: $Br(J/\psi\pi)/Br(J/\psi K) = (4.86 \pm 0.62) \times 10^{-2}$. However, this is not the case with the $J/\psi K^*$ signal, which falls only partially into the mass fit window. Its contribution depends to a large extent on the parametrization and on the accuracy of the corresponding Monte Carlo simulation. Moreover, other $B \rightarrow J/\psi X$ decays may contribute to the $J/\psi K^*$ signal in the mass fit window, which may make its contribution even more uncertain. The uncertainty in the $J/\psi K^*$ signal contribution was accounted in the systematic uncertainty of the measurement.

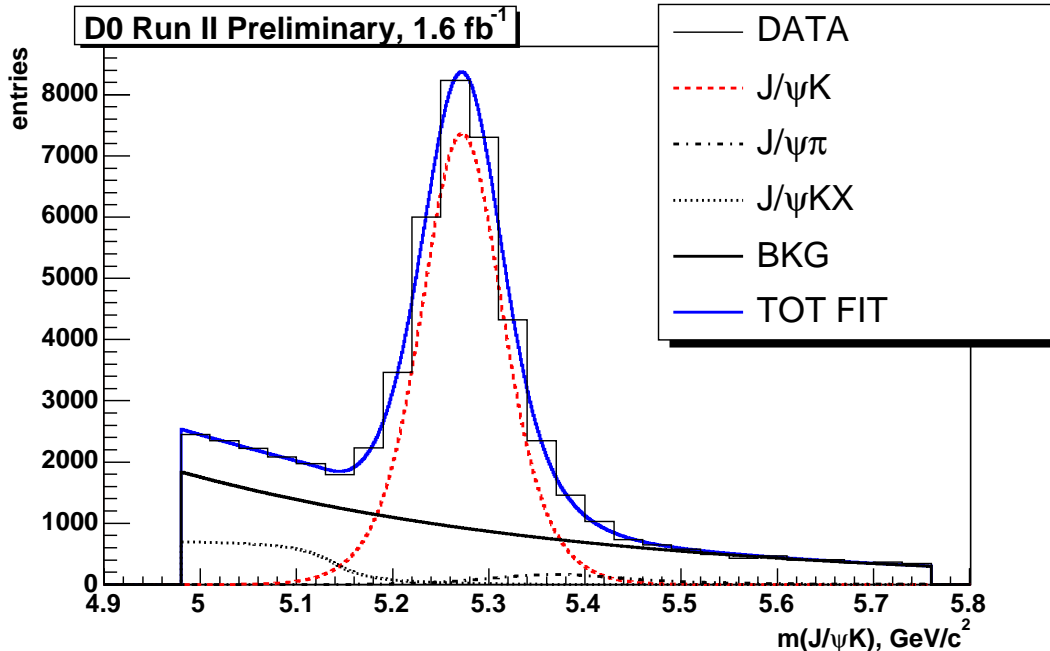


FIG. 2: Result from the unbinned fit of invariant mass distribution of the $J/\psi K$ system.

TABLE I: Result from the unbinned fit: number of events in each channel.

Channel	#events
$J/\psi K$	$27,700 \pm 201$
$J/\psi \pi$	$1,073 \pm 97$
$J/\psi K^*$	$3,759 \pm 181$
BKG	$21,932 \pm 351$
Total # of events in the signal region	54,464

V. A_{CP} MEASUREMENT

We need to measure the charge asymmetry between $B^- \rightarrow J/\psi K^-$ and $B^+ \rightarrow J/\psi K^+$ events:

$$A = \frac{N(B^- \rightarrow J/\psi K^-) - N(B^+ \rightarrow J/\psi K^+)}{N(B^- \rightarrow J/\psi K^-) + N(B^+ \rightarrow J/\psi K^+)}, \quad (2)$$

namely, the asymmetry between positive and negative kaons in the selected sample. However, the detector can introduce apparent charge asymmetries [9], which need to be disentangled. We used the method applied in Ref. [10].

To summarize, we exploited the reversal of magnet polarities of the D0 detector and divided the initial event sample into eight subsamples corresponding to all possible combinations of the magnet (toroid or solenoid) polarity $\beta = \pm 1$, the sign of the pseudorapidity of the charged particle $\gamma = \pm 1$, and the sign of the charge of the particle $q = \pm 1$. Then the physics and the detector can be modelled as follows:

$$n_q^{\beta\gamma} = \frac{1}{4} N \epsilon^\beta (1 + qA)(1 + q\gamma A_{fb})(1 + \gamma A_{det}) \times (1 + q\beta\gamma A_{q\beta\gamma})(1 + q\beta A_{q\beta})(1 + \beta\gamma A_{\beta\gamma}). \quad (3)$$

Here N is the total number of signal events; ϵ^β is the fraction of signal events with magnet (toroid or solenoid) polarity β ($\epsilon^+ + \epsilon^- = 1$); A is the physics charge asymmetry to be measured; A_{fb} is the forward-backward asymmetry; A_{det} is the detector asymmetry for particles emitted in the forward and backward direction; $A_{q\beta\gamma}$ accounts for the change in acceptance of particles of different sign bent by the magnet in different directions; $A_{q\beta}$ is the detector asymmetry which accounts for the change in the particle reconstruction efficiency when the magnet polarity is reversed; $A_{\beta\gamma}$

TABLE II: Number of events in the $J/\psi K$, $J/\psi\pi$, $J/\psi K^*$, and background channels in different $\beta\gamma q$ subsamples. All uncertainties are statistical.

$\beta\gamma q$	$J/\psi K$	$J/\psi\pi$	$J/\psi K^*$	BKG
+++	$3,376 \pm 70$	209 ± 35	455 ± 62	$2,579 \pm 122$
+ - +	$3,399 \pm 70$	185 ± 35	524 ± 63	$2,535 \pm 123$
++ -	$3,343 \pm 70$	149 ± 33	532 ± 63	$2,524 \pm 122$
+ - -	$3,369 \pm 70$	47 ± 29	340 ± 64	$2,856 \pm 121$
- + +	$3,546 \pm 73$	129 ± 34	444 ± 66	$2,998 \pm 127$
- - +	$3,626 \pm 73$	89 ± 32	436 ± 66	$2,941 \pm 126$
- + -	$3,467 \pm 71$	205 ± 34	552 ± 64	$2,651 \pm 124$
- - -	$3,565 \pm 71$	67 ± 33	476 ± 65	$2,840 \pm 124$
#tot	$27,700 \pm 201$	$1,073 \pm 97$	$3,759 \pm 181$	$21,932 \pm 351$

TABLE III: Physics asymmetry A and detector asymmetries for different channels after solving the system (3). All uncertainties are statistical.

	$J/\psi K$	$J/\psi\pi$	$J/\psi K^*$	BKG
N	$27,694 \pm 202$	$1,097 \pm 94$	$3,763 \pm 180$	$21,926 \pm 351$
ϵ^+	0.4871 ± 0.0036	0.5368 ± 0.0586	0.5053 ± 0.0198	0.4747 ± 0.0038
A	-0.0072 ± 0.0073	-0.1890 ± 0.1168	0.0035 ± 0.0498	-0.0075 ± 0.0160
A_{fb}	-0.0009 ± 0.0073	0.2192 ± 0.1160	0.0089 ± 0.0494	-0.0285 ± 0.0160
A_{det}	-0.0081 ± 0.0073	0.3333 ± 0.1060	0.0590 ± 0.0497	-0.0196 ± 0.0160
$A_{q\beta\gamma}$	0.0006 ± 0.0073	0.0354 ± 0.1228	0.0571 ± 0.0497	-0.0065 ± 0.0160
$A_{q\beta}$	0.0027 ± 0.0073	-0.2307 ± 0.1170	-0.0176 ± 0.0498	0.0319 ± 0.0160
$A_{\beta\gamma}$	0.0045 ± 0.0073	-0.0027 ± 0.1145	0.0335 ± 0.0496	-0.0071 ± 0.0160

accounts for any detector related forward-backward asymmetries that remain after the magnet polarity flip. Equation (3) expresses the fact that the number of events in each $\beta\gamma q$ subsample deviates from $\frac{1}{4}N\epsilon^\beta \approx \frac{1}{8}N$ due to physics charge asymmetry A , and various detector asymmetries. By solving (3) we disentangle the detector asymmetries by actually measuring them together with the physics charge asymmetry.

The procedure described was used to measure the charge asymmetry A . The initial sample was divided into eight subsamples corresponding to eight combinations of the solenoid polarity, kaon pseudorapidity and kaon charge. The invariant mass distribution of the $\mu\mu K$ system in every subsample was fitted, and the number of events in the $J/\psi K$, $J/\psi\pi$, and $J/\psi K^*$ channels extracted (see Table II).

All parameters of the fits apart from the fractions of the $J/\psi K$ signal, the $J/\psi\pi$ signal, and the $J/\psi K^*$ signal, were fixed to the values determined from the fit to the whole sample. The system of simultaneous equations (3) was solved with MINUIT for all channels. The resulting asymmetries are shown in the Table III. The measured charge asymmetry is $A = -0.0072 \pm 0.0073(stat)$.

Note that the number of events in $J/\psi\pi$ channel considerably fluctuates between the different $\beta\gamma q$ subsamples (see Table II), so the charge asymmetry measured in this channel, $A_{CP}(B^+ \rightarrow J/\psi\pi^+) \approx -0.19 \pm 0.12(stat)$, as well as the detector asymmetries, are subject to high systematic uncertainty due to the fitting procedure and background description. The number of events in $J/\psi K^*$ channel also undergoes fluctuations, although at a lower level. The effect of those fluctuations on the determination of CP violating asymmetry in the $J/\psi K$ channel was accounted for in the systematic uncertainty from the likelihood fit parametrization of the $J/\psi\pi$ and $J/\psi K^*$ signals.

VI. KAON ASYMMETRY

In the process we study, a single kaon is produced in the final state. Positive and negative kaons have different inelastic cross-section with the detector material: $\sigma(K^- d_{inelastic}) > \sigma(K^+ d_{inelastic})$ [8]. This difference is due to existence of Y hyperons: reactions $K^- N \rightarrow Y\pi$ have no $K^+ N$ analog. Therefore the average path of K^+ -s in the detector is longer than that of K^- 's, which results in higher reconstruction efficiency of K^+ -s and a visible positive asymmetry

$$A_K = \frac{N(K^+) - N(K^-)}{N(K^+) + N(K^-)} > 0. \quad (4)$$

This asymmetry adds to any charge asymmetry due to the Standard Model or possible Beyond the Standard Model processes. This is an integrated effect which depends on the number of radiation lengths exposed to kaons in different directions from the interaction point, and is detector-dependent.

We measured this kaon asymmetry in DØ detector using a sample of $c \rightarrow D^{*+} \rightarrow D^0 \pi^+$, $D^0 \rightarrow \mu^+ \nu K^-$ and charge conjugate events selected from 1.3 fb^{-1} of RunII D0 data. The D^0 candidate was reconstructed from the muon track by adding another track, which was assigned a kaon mass. The invariant mass of the two tracks was required to be in the window $1.0 < m(\mu K) < 2.2$.

The D^* candidate was reconstructed by adding a third track associated with the same primary vertex as the muon. It was assigned the mass of a pion. The invariant mass of the $\mu K \pi$ system was computed and the mass difference $\Delta m = m(\mu K \pi) - m(\mu K)$ was required to be $\Delta m < 0.22 \text{ GeV}/c^2$. Then, to match the D^* event topology, the sample of “right” charge correlation events was selected requiring $q_\mu \cdot q_K < 0$ and $q_\mu \cdot q_\pi > 0$. The Δm distribution of “right” events is shown on the Fig. 3 for different $m(\mu K)$ bins which span the range $1.2 < m(\mu K) < 1.9 \text{ GeV}/c^2$ around the D^0 peak in the $m(\mu K)$ distribution. The D^* peak is clearly visible.

To describe the background under the D^* peak the sample of “wrong” charge correlation events was selected by requiring $q_\mu \cdot q_K > 0$ and $q_\mu \cdot q_\pi > 0$. In every $m(\mu K)$ bin the signal band was defined to be $(\Delta m_1, \Delta m_2)$, where Δm_1 marks the beginning of the Δm distribution, near the $m(D^{*+}) - m(D^0)$ threshold, and Δm_2 was chosen in each $m(\mu K)$ bin separately to maximize the signal significance $S/\Delta S$, S to be defined below. The sideband was arbitrarily chosen to be $(0.19, 0.22)$, since the systematic effect from its choice is negligible. Let N_{wrong}^{sig} and N_{wrong}^{side} be the number of events in the signal and the sidebands of the Δm distribution of the wrong charge correlation sample, and N_{right}^{sig} and N_{right}^{side} - the same numbers for the right charge correlations sample. Then the number of background events under the D^* peak was defined from the sideband as

$$B = \frac{N_{wrong}^{sig}}{N_{wrong}^{side}} \cdot N_{right}^{side}, \quad (5)$$

and then subtracted from the total number of events in the D^* peak to give the pure signal:

$$S = N_{right}^{sig} - B. \quad (6)$$

The kaon asymmetry was measured as a charge asymmetry of an associated muon in a D^* event: $A_K = -A_\mu$. To disentangle the detector-induced asymmetries the technique described in the previous section was used. The initial sample was divided into eight subsamples according to the muon charge, muon pseudorapidity, and toroid polarity, and the “per $m(\mu K)$ bin” sideband subtraction (6) was performed in each subsample to determine $n_q^{\beta\gamma}$. Then the system (3) was solved for all asymmetries, including the muon charge asymmetry.

In addition, the dependence of the kaon asymmetry on the kaon momentum, p_K , was measured in p_K bins of approximately equal statistics, see Fig. 4. The kaon asymmetry was found to be maximal at low $p_K \sim 1 \text{ GeV}/c$ and to decrease as expected, due to $\sigma(K^+ d_{total}) \approx \sigma(K^- d_{total})$ at $p_K \gtrsim 10 \text{ GeV}/c$ [8]. The kaon asymmetry in the $J/\psi K$ events was found by convolving the D^* -measured kaon asymmetry with the pdf of the kaon momentum in the $J/\psi K$ sample:

$$A_K = \sum_{i=1}^{N_{p_K \text{ bins}}} A_{K,i}(D^*) \frac{N_i(J/\psi K)}{N(J/\psi K)}, \quad (7)$$

where $A_{K,i}(D^*)$ is the kaon asymmetry measured in i -th p_K bin in the D^* sample, $N_i(J/\psi K)$ - the number of $J/\psi K$ events falling into the i -th p_K bin, $N(J/\psi K)$ - the total number of $J/\psi K$ events, and the sum is performed over the p_K bins. The numbers $N_i(J/\psi K)$ were determined from the unbinned fit in each p_K bin. The kaon asymmetry in our $J/\psi K$ sample was measured to be $A_K = 0.0139 \pm 0.0013(stat)$. The CP violating asymmetry is then $A_{CP} = A + A_K$, where A is the measured charge asymmetry between B^+ and B^- .

VII. SYSTEMATIC UNCERTAINTIES

The systematic uncertainty on A_{CP} originates from the systematic uncertainties on the measured charge asymmetry A and on the kaon charge asymmetry A_K .

There are two important sources of the systematic uncertainty on A : the uncertainty from the unbinned fit procedure, and the uncertainty from the likelihood fit parametrization of the $J/\psi \pi$ and $J/\psi K^*$. The uncertainty from the fit procedure was estimated as follows. A number of parameters have been determined with a certain accuracy from

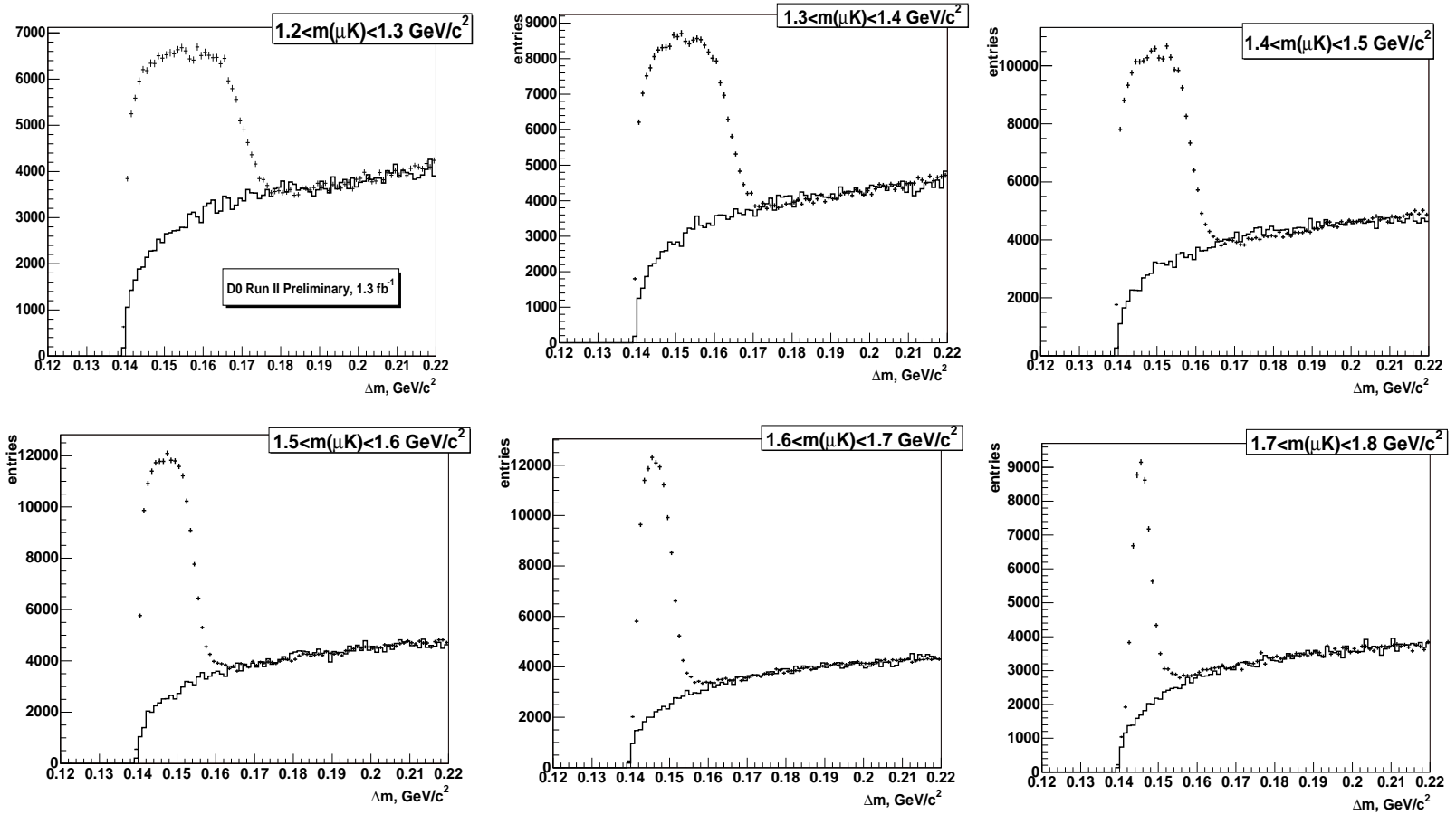


FIG. 3: The Δm distributions of D^* events in different $m(\mu K)$ bins for the samples of “right” (points) and “wrong” (solid line) charge correlation events. Note that the optimal value of Δm_2 differs for different $m(\mu K)$ bins. The background distribution is rescaled to fit the tail of the signal distribution for visual clarity.

TABLE IV: Variation of the fit parametrization: changes in the parametrization of the $J/\psi\pi$ and $J/\psi K^*$ contributions. The nominal value of A is -0.0072 .

Fixing	$A(J/\psi K)$	$A(J/\psi\pi)$	$A(J/\psi K^*)$	$A(\text{BKG})$
$J/\psi K^*$ fraction $\rightarrow 0$	-0.0079	-0.2098	$-$	0.0043
$R_{J/\psi\pi} \rightarrow$ “all” value	-0.0078	0.0488	-0.0581	0.0198
$R_{J/\psi K^*} \rightarrow$ “all” value	-0.0077	-0.1847	0.0035	0.0041
$R_{J/\psi\pi}, R_{J/\psi K^*} \rightarrow$ “all” value	-0.0098	-0.0086	0.0077	0.0076

the unbinned fit in the whole sample and fixed when unbinned-fitting in the subsamples. The uncertainty on these parameters was propagated to the systematic uncertainty by varying each parameter by $\pm 1\sigma$.

The systematic uncertainty from the $J/\psi\pi$ and $J/\psi K^*$ parametrization was estimated as follows. First, to determine the systematic effect from the uncertainty on the $J/\psi K^*$ signal contribution, we fixed the fraction of the $J/\psi K^*$ signal to zero and repeated the fit. Second, to determine the systematic effect of the asymmetry in the $J/\psi\pi$ and $J/\psi K^*$ channels, we artificially suppressed the asymmetry in the $J/\psi\pi$ channel, then in the $J/\psi K^*$ channel, then in both as follows. We determined the ratio R of the $J/\psi\pi$ ($J/\psi K^*$) signal fraction to the background fraction from the fit in the whole sample and repeated the fits in the subsamples keeping this ratio fixed to the “all” fit value. The variations of the charge asymmetry in the $J/\psi K$ channel, $A(J/\psi K)$, are summarized in Table IV, together with the variations in other channels. The maximum variation of $A(J/\psi K)$ from the nominal value was used as an estimate of the systematic uncertainty on A from the $J/\psi\pi$ and $J/\psi K^*$ parametrization.

The systematic uncertainty on A_K originates from the unknown reconstruction efficiency of some modes contributing to the D^* sample. This produces an uncertainty on the D^* sample composition which propagates into the uncertainty on the kaon asymmetry measurement. We recalculated the kaon asymmetry assuming 0% and 100% reconstruction efficiency of these modes and assigned a deviation from the average value as a systematic uncertainty from this effect. The systematic effect from choosing the sideband was found to be negligible.

The systematic uncertainties are summarized in Table V. The total systematic uncertainty was obtained by summing the contributions in quadrature. It is largely dominated by the likelihood parametrization uncertainty.

We also performed the following consistency check. We calculated $A_{CP}(B^+ \rightarrow J/\psi K^+)$ separately in two subsamples of events with kaon momentum $p_K < 4.2$ GeV/ c and $p_K > 4.2$ GeV/ c , in which the kaon asymmetry is correspondingly high and low, see Fig. 4, and the statistics is approximately the same. The result is shown in Table VI. The difference between two asymmetries is $\Delta A_{CP} = 0.0244 \pm 0.0158$, which is consistent with a statistical fluctuation.

VIII. RESULT

The charge asymmetry between $B^- \rightarrow J/\psi K^-$ and $B^+ \rightarrow J/\psi K^+$ was measured to be $A = -0.0072 \pm 0.0073(\text{stat}) \pm 0.0026(\text{syst})$. The kaon asymmetry in the $J/\psi K$ sample (7) was found to be $A_K = 0.0139 \pm$

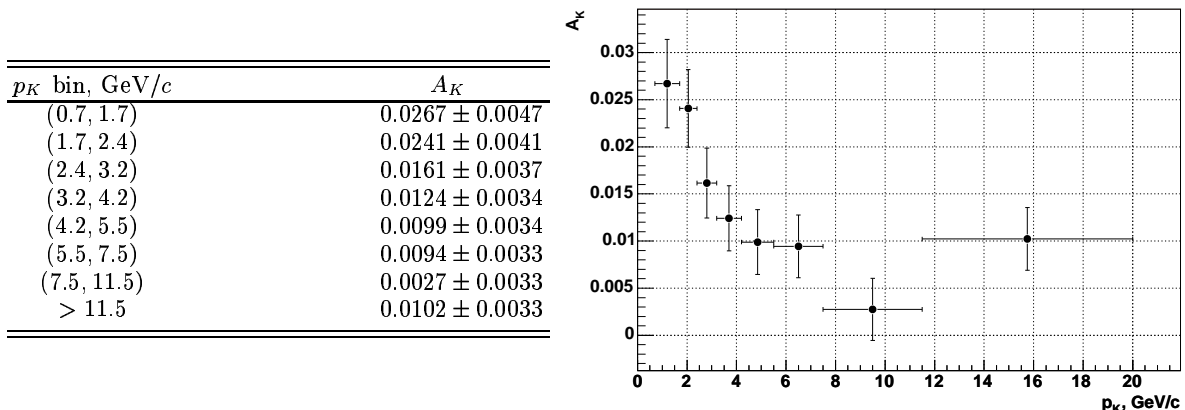


FIG. 4: Dependence of the kaon asymmetry on p_K in eight bins of approximately equal statistics. Errors are statistical.

TABLE V: The systematic uncertainties on A_{CP} .

from A:	
Unbinned fit procedure	0.0002
Likelihood parametrization of the $J/\psi\pi$ and $J/\psi K^*$ signals	0.0026
from A_K:	
Unknown reconstruction efficiency of some decay modes contributing to D^* sample	0.0004
Total:	0.0026

TABLE VI: $A_{CP}(B^+ \rightarrow J/\psi K^+)$ separately for $p_K < 4.2$ GeV/ c and $p_K > 4.2$ GeV/ c .

	A	A_K	A_{CP}
$p_K < 4.2$ GeV/ c	-0.0025 ± 0.0096	0.0201 ± 0.0021	0.0176 ± 0.0098
$p_K > 4.2$ GeV/ c	-0.0144 ± 0.0123	0.0076 ± 0.0015	-0.0068 ± 0.0124

0.0013(stat) \pm 0.0004(syst). Finally:

$$A_{CP}(B^+ \rightarrow J/\psi(1S)K^+) = +0.0067 \pm 0.0074(stat) \pm 0.0026(syst), \quad (8)$$

which is consistent with zero, but measured with a precision at the level of 1%, i.e. the A_{CP} predicted by the Standard Model. Our measurement is consistent with the PDG-2007 world average, $A_{CP}(B^+ \rightarrow J/\psi K^+) = +0.015 \pm 0.017$ [8], but has a factor of two better precision, thus providing the most stringent bounds for new models predicting large values of A_{CP} .

Acknowledgments

We thank the staffs at Fermilab and collaborating institutions, and acknowledge support from the DOE and NSF (USA); CEA and CNRS/IN2P3 (France); FASI, Rosatom and RFBR (Russia); CAPES, CNPq, FAPERJ, FAPESP and FUNDUNESP (Brazil); DAE and DST (India); Colciencias (Colombia); CONACyT (Mexico); KRF and KOSEF (Korea); CONICET and UBACyT (Argentina); FOM (The Netherlands); Science and Technology Facilities Council (United Kingdom); MSMT and GACR (Czech Republic); CRC Program, CFI, NSERC and WestGrid Project (Canada); BMBF and DFG (Germany); SFI (Ireland); The Swedish Research Council (Sweden); CAS and CNSF (China); Alexander von Humboldt Foundation; and the Marie Curie Program.

-
- [1] I. Dunietz, Phys. Lett. **B316**, 561 (1993).
 - [2] V. Barger, C.-W. Chiang, P. Langacker, H.-S. Lee, Phys. Lett. **B598**, 218 (2004).
 - [3] G.-H. Wu, A. Soni, Phys. Rev. **D62**, 056005 (2000).
 - [4] V. M. Abazov *et al* (D0 Collaboration), Nucl. Instrum. Methods A **565**, 463 (2006).
 - [5] V. M. Abazov *et al* (D0 Collaboration), Nucl. Instrum. Methods A **552**, 372 (2005).
 - [6] J. Abdallah *et al* (DELPHI Collaboration), Eur. Phys. J **C32**, 185 (2004).
 - [7] G. Borisov, Nucl. Instrum. Methods A **417**, 384 (1998).
 - [8] W.-M. Yao *et al* (Particle Data Group), J. Phys. G **33**, 1 (2006) and 2007 partial update for edition 2008 (URL: <http://pdg.lbl.gov>).
 - [9] V. Abazov *et al* (D0 Collaboration), Phys. Rev. D **74**, 092001 (2006).
 - [10] V. Abazov *et al* (D0 Collaboration), Phys. Rev. Lett. **98**, 151801 (2007).